MICROFABRICATION OF HETEROGENEOUS, OPTIMIZED COMPLIANT MECHANISMS

NSF Summer Undergraduate Fellowship in Sensor Technologies
Luo Chen (Mechanical Engineering) - University of Rochester
Advisor: G. K. Ananthasuresh

ABSTRACT

Metal deposition by electroplating has been extensively used and analyzed for industrial applications, but it remains insufficiently characterized for fabricating compliant micromechanisms. This research presents a new fabrication process for heterogeneous optimized compliant mechanisms that consists of placing two materials side by side as opposed to the convention of stacking materials layer by layer. The fabrication process uses standard bulk micromachining and electroplating techniques. This paper reviews and discusses the theory and method of electroplating for obtaining optimum structural and surface morphology. We also present a novel method for protecting a silicon wafer from wet etching using black wax. In fabricating these two-material mechanisms, we found that optimum microstructures can be obtained by electroplating at a low-current density while maximizing the reaction kinetics.

1. INTRODUCTION

1.1 Motivation

With recent progress in micromachining, manufacturers can build microdevices such as microelectromechanical systems (MEMS) using two or more materials without much difficulty. Designing them to operate at optimal performances is another issue, however. Many researchers have found that traditional engineering methods used to design and analyze macrostructures are effective for tackling micro-engineering problems. Topology optimization design methods, well known for solving problems in macrostructural engineering (e.g., designing structures with maximum stiffness), are currently being used systematically to design and tackle multi-material distribution problems in compliant micromechanisms. Current advances in topology optimization have demonstrated that fabricating a microactuator with two materials can increase the microactuator's performance (e.g., output displacement and stroke) [1]. Using two materials is not unprecedented in manufacturing microdevices, but the ones that have been built, such as the bimorph microactuators, have limitations.

Copper and nickel electrodeposition techniques onto silicon have been well characterized by the scientific community; however, gold electrodeposition onto silicon is not completely understood. Electroplating (one of the methods in electrodeposition) was established by the 19th-century scientist Michael Faraday, but it is only now becoming a standard technique used in micromachining MEMS. This recent appreciation is due to rising interest by engineers and scientists, who have been seeking an innovative microfabrication tool that promises a high rate of deposition, manageable scalability, and commensurability with current manufacturing

processes in microelectronics and microsystems research. Electroplating is emerging as this promising tool. Its popularity is well deserved, since researchers are discovering the method's cost advantages over conventional methods, notably evaporation and sputtering [2]. It appears that scientific progress can only be achieved by combining new and old methods; topology optimization designing and electroplating are two examples of scientific rediscovery and revivals.

The goal of the new fabrication process described in this paper is to manufacture a two-material compliant MEMS micromechanism, with emphasis on the side-by-side material distribution as conceptually shown in Figure 1. Currently, the common mechanical structures manufactured are either two-material, like the bimorph sandwich out-of-plane mechanism that is built layer by layer, or the one-material one, like the electrothermal in-plane mechanism. Figure 1 illustrates the need for a fabrication process that can combine features from both devices. Therefore, the motivation for the microfabrication process is to manufacture a two-material mechanical device that can be electrothermally actuated for in-plane motion.

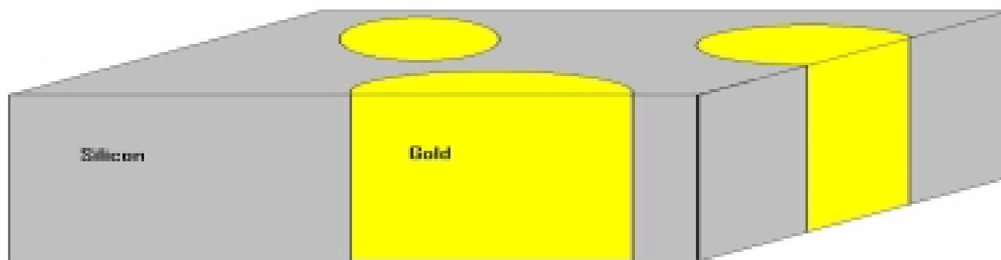

Figure 1: Islands of gold on silicon placed side by side.

The first step in the microfabrication process is to create a cavity on a silicon substrate, and then to electroplate gold onto the cavity. In this paper, the basics and theory of electroplating and method for obtaining high-resolution morphology are discussed. The last step is to open a window from the backside of the substrate with black wax and another window from the front surface of the substrate to suspend a two-material cantilever beam. First, we will discuss the background of some related research. The fabrication process is then discussed in subsequent sections.

1.2 Background of Related Work

1.2.1 Compliant MEMS

In recent years, microelectromechanical systems have received considerable attention from the engineering community. MEMS devices have stationary or moveable mechanical components with micron-size dimensions. The field of MEMS has many promising areas of application in the

aerospace, automotive, biotech, electronic, and healthcare industries. For example, microactuators, which are a type of MEMS devices, can perform micromanipulation tasks by converting thermal, electrostatic, mechanical, optical, electromagnetic, or electrical energy to some form of controlled motion. With their micromanipulating capability, MEMS microactuators can be a significant advancement in microsurgical tools, where accuracy is imperative for highly sensitive operations.

However, manufacturing and assembling MEMS devices with moveable components - i.e., bearings, hinges, and joints - can be very difficult given the limitations of the small dimensions standardized in these devices and the impracticality of the rigid-body mechanisms. These silicon-based microstructures are traditionally manufactured using a very-large-scale integration of microelectronic fabrication techniques from the integrated circuit industry. However, with increasing complexity in the design and function of MEMS devices, new fabrication processes are needed to reduce the complications of manufacturing and integrating them. Thus, in recent years, researchers have intuitively come up with a viable solution to the MEMS problem by implementing compliance in MEMS.

Compliant mechanisms are monolithic jointless devices made to deform flexibly in order to obtain useful work when actuated. These mechanical devices are designed to transfer or transform motion, force, or energy. Figure 2 is an example of a compliant mechanism known as the pantograph, built by Brigham Young University researchers. These pantographs are used to amplify force and motion at the micro level.

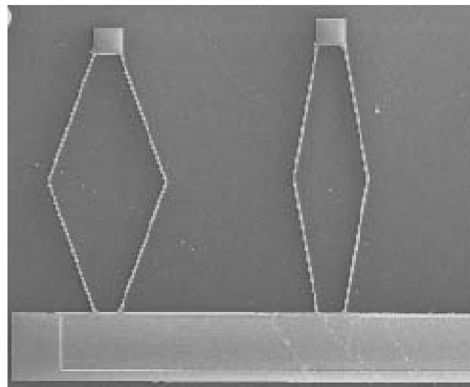

Figure 2: Compliant pantographs with MEMS applications.

Therefore, the introduction of compliant mechanisms in MEMS minimizes assembly problems from friction-induced wear and stress-related fractures.
Compliant MEMS can be advantageously manufactured in a single piece with microfabrication techniques using bulk and surface micromachining, which consist of etching or depositing layers of thin film materials onto a silicon substrate. Moulton and Ananthasuresh have shown that by controlling the topological and geometrical parameters of micromechanical structures, compliant microactuators can be built producing large displacements and forces [3].

1.2.2 Bimorph Effect

The impetus behind the fabrication of microactuators started with the work of S. Timoshenko, who proposed the theory of bending "sandwich" microstructures more than 70 years ago. His sandwich microstructure consists of two or more materials with different coefficients of thermal expansion (CTE) stacked on top of another. - His theory and the bilayer mechanical structure are known as the bimorph effect. Some of the materials used commonly in standard integrated circuit fabrication are also used in manufacturing thermal bimorph devices. Materials with high CTE - notably aluminum, nickel, gold, or chromium - are commonly stacked onto materials with low CTE - such as silicon, polysilicon, silicon dioxide, and silicon nitride [4]. Using gold and silicon, Riethmuller and Benecke have fabricated bimorph microactuators. They fabricated a two-material cantilever beam that is electrically driven by resistors sandwiched between the two materials [5]. These bimorph actuators produce out-of-plane deflections upon differential expansion of the two materials. In our research, gold and silicon are also used to fabricate compliant mechanisms. Sandwich microactuators generally provide large forces and deflections of as much as 100 μm [6]. Therefore, these devices have found various MEMS applications such as its use in electrical switches [5].

Mismatch of the coefficient of thermal expansion in bimorph microactuators, between two or more materials stacked layer-by-layer, presents several problems that are well understood in the MEMS community. CTE mismatch can lead to internal stress buildup in the MEMS structure, which can be a problem for the reliability of the device. Furthermore, these microactuators have shortcomings in out-of-plane deflections where the large radius of curvature has found to be incompatible with some MEMS applications [4]. Thus, to avoid these problems, researchers have designed electrothermal microactuators as an alternative to sandwich microactuators. Electrothermally actuated microdevices have been fabricated recently with one material and found to operate as a pseudo-bimorph effect. This discussion and the next section introduce the value behind this new microfabrication process for compliant mechanisms that are electrothermally actuated and broach the motive for and background of devices that employ the principles of the pseudo-bimorph effect.

1.2.3 Electro-Thermal-Compliant Microactuators

With their capability for micromanipulation, electrothermal microdevices - particularly compliant microactuators - have received considerable attention, especially for their ability to generate force in the millinewton range and create in-plane displacements of several microns or more [3]. A class of electro-thermal-compliant (ETC) microactuators known as heatuators, which behaves with the pseudo-bimorph effect, will be used as an example to discuss and differentiate the purpose of this research. Current heatuators are one-material compliant mechanisms that are actuated to create in-plane motion.

The design and modeling of ETC heatuators can be traced to the work of former SUNFEST student T. Moulton. His research motivated many people and projects, including this one. Figure 3 shows an earlier version of the ETC heatuator that Moulton built [3]. This microactuator can be actuated by applying a voltage through the anchors of a cantilever beam with two arms of different widths. Actuation of this single-material micromechanical structure can be attained

with current passing through the device. By virtue of the unique shape, the narrow arm becomes hotter and deflects down, bending toward the wide arm and thus creating in-plane lateral motion [7]. Recent progress in MEMS modeling has shown that the deflection of the microactuator tip can be explained with finite element analysis of the structure through assessment of the current and temperature distribution, and thermal boundary conditions in the microactuator [3, 7, 8]. These models show that higher resistance is distributed in the narrow arm than in the wider arm, which results in the microactuator tip moving laterally. This disparity in resistance can be attributed to non-uniform thermal expansion in the two arms from non-uniform Joule heating. Therefore, the operating principle behind ETC microactuation and the elastic deformation of these ETC devices are based on the constrained thermal expansion of a flexible continuum of material(s) created by internal Joule heating of the micromechanical structure [8].

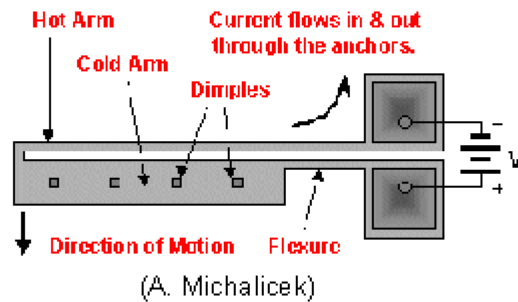

Figure 3: Electrothermally actuated heatuator made for in-plane motion.

Recently, Moulton and Ananthasuresh designed and fabricated a silicon-based ETC heatuator, as shown in Figure 4. This heatuator has two arms of equal widths, one arm is selectively doped but the other is not. Because selective doping changes the resistivity of a material, each arm in the heatuator has a different value of resistance when current passes through it [3]. Like the basic heatuator of unequal widths mentioned earlier, the selectively doped heatuator works under the principle of non-uniform joule heating accompanied by thermal expansion. This single-material compliant mechanism acts like a two-material device.

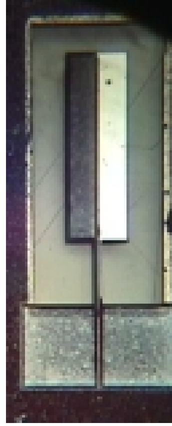

Figure 4: Selectively doped ETC heatuator.

1.2.4 Topology Optimization of Two Materials

Riethmuller and Benecke's design of the sandwich thermal microactuator came partly from intuitive guessing and partly from scientific reasoning building upon Timoshenko's bimorph effect. Similarly, J. Comtois and V. Bright based their intuitive design for heatuators on a modification of H. Guckel's earlier version. Designing such mechanisms with intuition can be conceptually difficult and time consuming. A more efficient method is needed. Since intensive research is currently taking place in MEMS, engineers have been given the opportunity to devise new design techniques as well as review older ones. In reviewing the topology optimization technique, engineers have realized that this method simplifies the MEMS designing process.

Topology optimization, which avoids the need to come up with new designs based on intuition, is a numerical method that requires the implementation of a finite element method algorithm. The purpose of the topology optimization algorithm in this type of research is to design a compliant mechanism such as an ETC microactuator that can optimally distribute materials given. Jonsmann, Sigmund, and Bouwstra have shown that electrothermally actuated micromechanisms designed with topology optimization have clear-cut performance advantages (e.g., increases in stroke and deflection) over micromechanisms that are not designed with this method [9].

Therefore, the next logical step in MEMS design of ETC mechanisms is to use topology optimization in constructing two-material devices that will take advantage of the compliance objective function. Yin and Ananthasuresh have shown that by specifying the conditions for a structure supported on its boundaries and subjected to given loads and constraints, one can optimize the compliance objective function by maximizing the mechanical and geometrical efficiency of a structure [10, 11]. Furthermore, by applying forces or voltage between two points on the device to obtain a desired output of displacements, one can generate a topology and shape that can provide the optimal distribution for a given amount of material. This optimum shape will be the solution for a multi-material thermally actuated compliant micromechanism.

Sigmund has demonstrated that one can significantly improve the performance of a one-degree-of-freedom device by using topology optimization of two-material microactuators [1]. He simulated a topology-optimized microactuator made from two materials that has gripping capability. The objective function of his method is to maximize the work done by the spring, while placing constraints on the resistance. Sigmund discovered that by introducing a material with a thermal conductivity half the value of the other material, one can obtain a micro-gripper that performs more than one-half times better than the one-material micro-gripper.

Using the Fortran 90 programming language, Yin and Ananthasuresh have also generated several two-material designs for ETC mechanisms. They use a multi-criteria objective function that requires an ETC micromechanism to produce maximum output displacement of the two-material structure - such as the ones shown in Figures 5a and 5b. Multi-material compliant mechanisms have been shown to perform better than current single-material ones using such simulations. Figures 5a and 5b display two compliant devices with different distribution of materials. The blue (or lighter) color and red (darker) color represent two materials with varied electrical conductivity, modulus of elasticity, thermal conductivity, and thermal expansion coefficient. In this device, the objective is to maximize the downward displacement of the centerpieces given dissimilar amount of materials. Figures 5c and 5d show the different temperature distribution in the compliant devices.

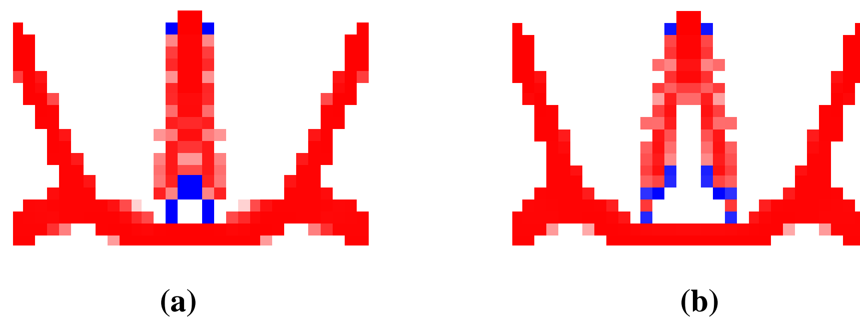

Figure 5a and 5b: Topology optimized, compliant micromechanism of two materials under electrothermal actuation (modeled with convection).

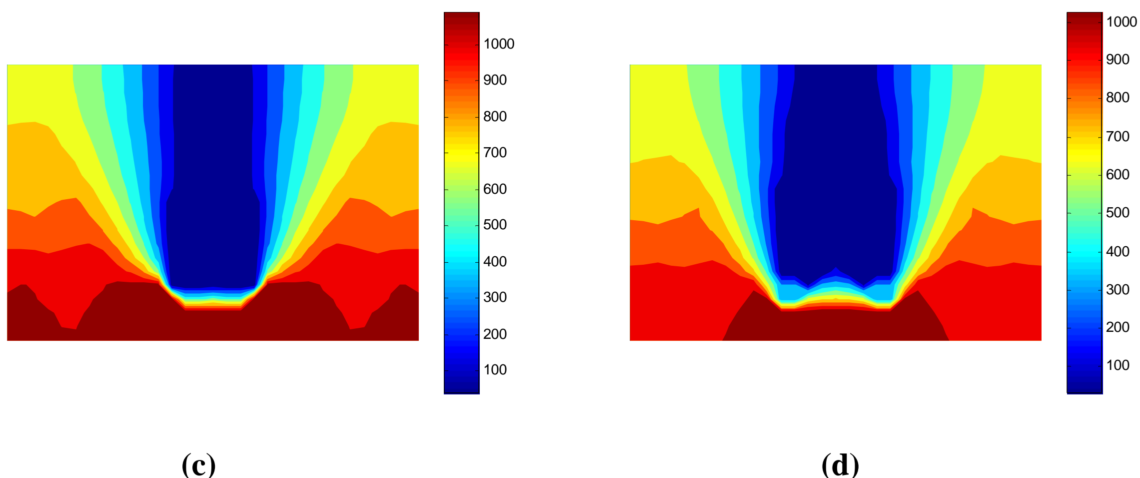

Figure 5c and 5d: Temperature distribution of micromechanisms from Figures 5a and 5b.

2. FABRICATION PROCESS

In order to fabricate the two-material compliant micromechanisms shown in Figure 5, a new fabrication process is needed. This process can typically begin with constructing a cavity on a silicon substrate to allow side-by-side placement of materials, similar to the conceptual idea presented in Figure 1. Making a cavity on a substrate requires a standard MEMS fabrication process known as bulk micromachining. This process consists of several fabrication techniques that involve removal of a designated portion of the silicon substrate. The fabrication techniques used in this bulk micromachining process consists of lithography, two masking layers, and wet chemical etching in order to carve out the preferred structure. After bulk micromachining, the process known as electron beam evaporation of the seed layer is used. The evaporation method is an intermediary step leading to the main fabrication step of the research: electroplating. Electroplating theory and procedures are discussed in the next sections.

2.1 Creating a Cavity on Silicon Wafer

The Silicon-on-Insulator (SOI) (manufactured by BCO Technologies) is a 4-inch, p-type wafer with <100>-crystal orientation. The SOI has a total thickness of 525 µm, consisting of a 20-µm-thick silicon device layer that has been mechanically and chemically polished, a 5-µm-thick silicon dioxide layer, and a 500-µm-thick unpolished silicon substrate. The SOI also has a silicon dioxide layer that will serve as an etch-stop layer. Figure 6 depicts the standard bulk micromachining process used in this fabrication process.

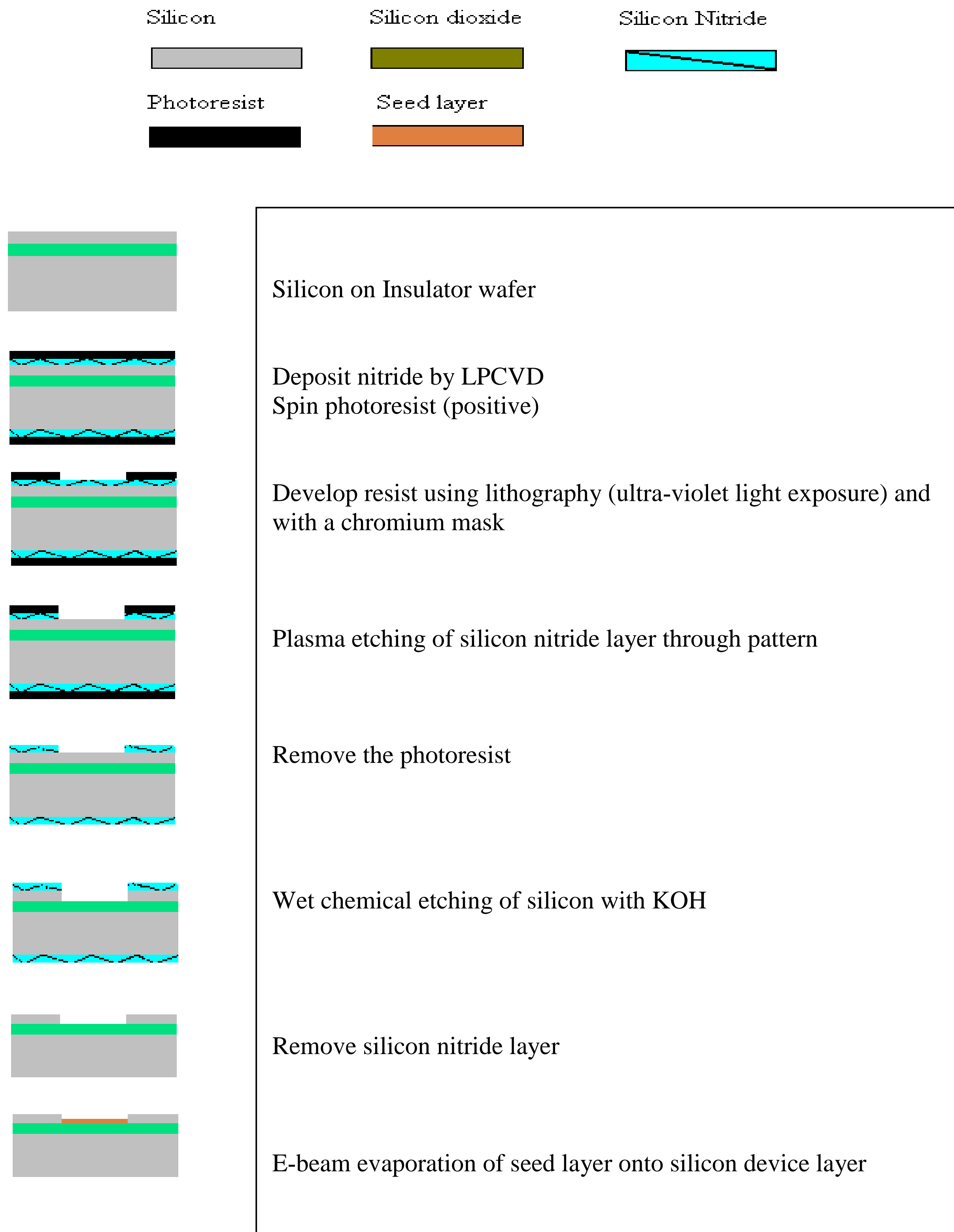

Figure 6: Schematic of bulk micromachining and e-beam processes used to create cavity on substrate.

In order for any adhesion to occur between the gold deposits and silicon substrate, a thin Nichrome layer and a subsequent gold layer are needed; these two combine to form the seed layer. Since gold adheres poorly to silicon, the crucible heating technique known as electron-beam (e-beam) evaporation is used to deposit the seed layer. In this technique, a high-energy electron source bombards and boils the wafer surface that is mounted on a crucible inside a bell-shaped chamber [12]. The e-beam process is used rather than the resistive or inductive evaporator systems because the other two processes can create charge contamination during the heating of the crucible. Furthermore, high deposition rates obtained with e-beam can be ~10 times faster than chemical vapor deposition or sputtering of the seed layer [6].

2.2 Principles of Electrodeposition

The magnitude of the overpotential as well as the reaction kinetics in an electrochemical cell can characterize the electroplating rate and determine the optimum morphology of the plated metal. The basic principles behind the plating model are discussed below.

The basic concepts of metal deposition can be explained with Faraday's laws of electrolysis. During electrolysis, when a current is applied, the ions in the solution react with the electrode by receiving or giving up electrons. Faraday's law predicts that the amount of the deposited material is a function of the current passing through the electrode interface and proportional to the chemical equivalent weight of the material [13]. The deposition rate can be determined from Faraday's Law, which is presented mathematically in the following way [2]:

$$M = \alpha \frac{I\,t\,A_W}{n\,F} \tag{1}$$

or

$$\frac{h}{t} = \alpha \frac{j\,A_W}{nF\rho} \tag{2}$$

where M = the mass of the deposited material (g)
α = current efficiency at the cathode
I = the total current (A)
t = the duration of electroplating (s)
n = the number of electrons transferred per atom in reduction reaction
F = Faraday's constant (9.65×10^4 C/mole)
h = the thickness of deposit (μm)
A = the area of deposit (cm)
ρ = the density of the deposit (g/cm^{3})
A_w = the atomic weight
j = the current density (mA/cm^2).

Here, the experimental case of *vertical static electrode* is presented for electrodeposition. This case is the most common form of setup for electroplating because it is relatively easy to put together. Figure 7 shows a diagram of the general setup for the vertical static electrode case. Other common forms of electrode setup are the horizontal electrode with laminar flow of

solution and the rotating disk electrode with laminar flow of solution. Each electrode-system setup has its own advantages and disadvantages. The placement of electrodes can change the thickness of the diffusion region and the limiting current density, as well as determine whether the flow of the electrolyte is by natural or forced convection [13].

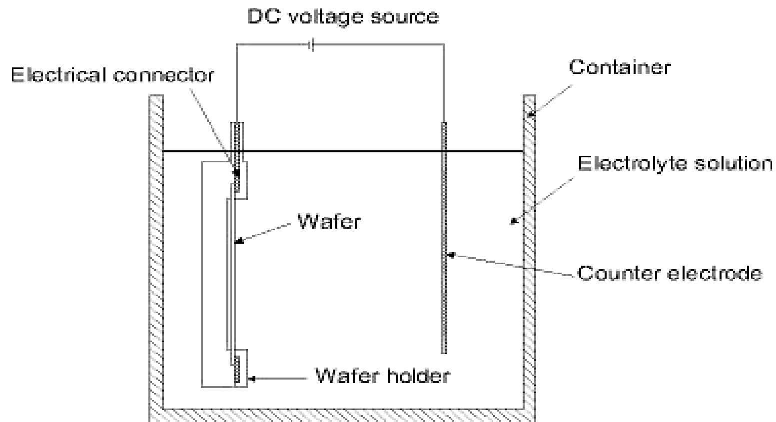

Figure 7: Vertical static electrode setup of electrochemical cell.

A model of what occurs in the electrochemical cell for the vertical static electrode case during electroplating is as follows. When plating a metal onto the silicon substrate (in this case, at the cathode) and before applying an external voltage across the cathode, there exists a potential between the cathode and the ions in the aqueous solution. As a consequence of this potential distribution, the ions migrate in the bulk solution toward the electrodes, creating regions with different chemical interfaces [13]. The positive ions react with the electrode at the metal-electrolyte interface either by receiving or giving up electrons. At this interface, since ions have electrical charges, they align along the substrate surface of the cathode, forming a dense layer of ions known as the Helmholtz (or electrical) double layer [14]. When an external voltage is applied across the electrochemical cell, the potential changes from its equilibrium value by an amount designated by the overpotential [15]. To provide sufficient energy for the charge transfer reaction and the charging of the Helmholtz double layer at the metal-electrolyte interface, electroplating requires a current passing through the electrodes. Whether the ions have enough energy to overcome the activation energy barrier and move across the Helmholtz layer to the cathode depends on the magnitude of the overpotential [14]. The overpotential can be defined as the excess voltage applied above the limiting current density, where the cell potential departs from its equilibrium value [6]. Therefore, controlling the magnitude of the overpotential of a chemical reaction is important. The overpotential is calculated using the following relationship:

$$\eta = E_{cell} - E \qquad (3)$$

where η = overpotential in volts
E_{cell} = potential when current is flowing in the cell
E = cathode potential represented by the Nernst Equation in volts

The Nernst Equation defines the equilibrium setup between the metal and its ions in the electrolyte as a function of the ion concentration for the products and reactants [15]. The relationship is given as follows:

$$E = E^\circ + \frac{RT}{nF} \ln \frac{[\text{products}]}{[\text{reactants}]} \qquad (4)$$

Where E° = standard electrode potential
R = gas constant
T = absolute temperature
n = number of electrons transferred
F = Faraday's constant

In an electrochemical cell, there also exists a diffusion region known as the Gouy-Chapman layer next to the Helmholtz double layer; electrical forces and natural transport effects of thermal convection are responsible for its existence, as shown in Figure 8 [13]. At the diffusion region, the ion concentration is less than equilibrium value [14]. Furthermore, with the concentration gradient across the diffusion region because of reduction at the cathode, the metal ions in the electrolyte are driven to deposit on the cavity on the silicon substrate.

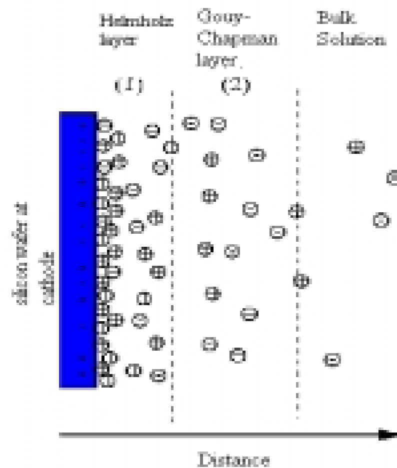

Figure 8: Model showing the effects of convection and diffusion on an electrochemical cell.

2.3 Method of Electrodeposition

Three basic electroplating techniques are used in metal deposition. These techniques provide energy to the electrochemical cell by means of constant current (galvanostatic or direct current [dc]), constant voltage (potentiostatic), or periodic reversal of current or voltage (pulse electroplating) [13]. The experiments conducted in this research use galvanostatic plating

techniques. Constant current has a few advantages over the other two techniques. One is in calculating the total current used in electroplating. The dc plating method avoids complications in the calculation of the total current term found in Faraday's Laws of Electrolysis. In general, the total current I_t passing through an electrode during metal deposition depends on the Faradic I_f and Helmholtz double layer components I_{dl} in the following way:

$$I_t = I_f + I_{dl} \quad (5)$$

Therefore, one must find the experimental value for both terms in equation (5) in order to calculate the total current. Thus, when plating at constant current in steady state the second term in equation (5) can be assumed to be insignificant and thus can be approximated to be zero [15]. In general, this technique is easier to control than pulse plating, especially when electroplating is done over a long period.

In the experimental setup, the electrochemical cell consists of the following components: silicon-on-insulator wafer (cathode), stainless steel plate (counter electrode), aqueous gold solution (electrolyte), and Hewlett Packard DC power supply. The plating solution used is Pure Gold SG-10 (Transene, Inc.). In a typical gold (Au) solution containing cyanide (CN) [6], the reaction consists of a fast equilibrium:

$$Au(CN)_2^{-} \leftrightarrow AuCn + CN^{-} \quad (6)$$

and a slow charge transfer reaction at the cathode:

$$AuCN + e^{-} \rightarrow Au\,(s) + CN^{-}. \quad (7)$$

The rate of a reaction is determined by the slowest step, which is the rate-determining step. In this case, the rate-determining step is the second equation, which is also the half-cell (reduction) reaction at the cathode.

While holding several electrodeposition process parameters constant, we varied the conditions of one parameter at a time. The parameters are the electroplated area, the current density, process temperature of cell, spacing between electrodes, agitation, concentration of metal ions, and the pH. Because of time constraints in this project, the last two parameters were not tested. Variations in the pH and concentration may have a strong impact in hydrogen evolution [6]. Testing and characterizing the effect of these parameters is important for obtaining acceptable morphology for micromachining, and this work should be done in the future work. In this research, we tried the following current applications: 1, 1.5, 2, 3.3, 5, and 10 mA.

Other operating conditions to be noted are that each cavity area is about 0.52±0.01 cm^2, electroplating occurred at room temperature (~20° C) and 60° C (the optimum plating temperature suggested by the manufacturer), and the electrodes are spaced apart at a constant distance of about 3 cm. In order to maintain a constant electroplated area, the wafer clamps are kept above the gold solution. One other concern in electroplating is the amount of hydrogen gases evolving. As acidified water becomes electrolyzed, these hydrogen gases are produced at the cathode because hydrogen ions receive electrons. During electrolysis, water is decomposed

in the redox reaction, where oxidation occurs at the anode and reduction at cathode [16]. These are the redox reactions:

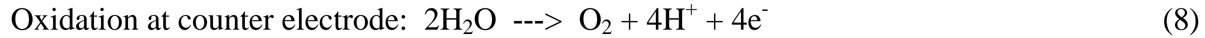

Oxidation at counter electrode: $2H_2O \dashrightarrow O_2 + 4H^+ + 4e^-$ (8)

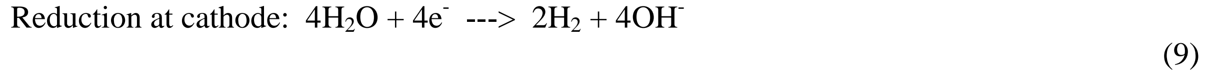

Reduction at cathode: $4H_2O + 4e^- \dashrightarrow 2H_2 + 4OH^-$ (9)

Since hydrogen gas created from water during electroplating requires energy (e.g., breaking bonds of water during electrolysis), we do not want it to compete with the current used for plating gold.

To find the optimum morphology, we vary one parameter at a time while holding the others constant and then compare the effect of each parameter by using a stylus profilometer. The profilometer measures the sharp steps of the surface profile for the gold film. Since the profilometer has viewing limitations, the scanning electron microscope is also used to examine the topography of the gold film on the silicon substrate. The results of electroplating are presented and discussed in section 3.

2.4 Wet Chemical Etching

This research presents a new method and material for protecting the fabricated microstructure. To release the two-material structure, we need to chemically etch the backside of the silicon wafer with a KOH solution, as portrayed in Figure 9. We also prefer to obtain similar quality surface results using black wax as the mask rather than the more commonly used silicon nitride. Figure 10 depicts the heating and application of black wax with pressure over the silicon surface and backside. The substrate is then mounted on the glass substrate. Then, a 10 mm by 6 mm window is sketched over the black wax to allow the KOH to etch only the area designated by the window. The KOH solution is aqueous; it contains 29% KOH by weight. In this experiment, the silicon substrate was etched at about 65° C.

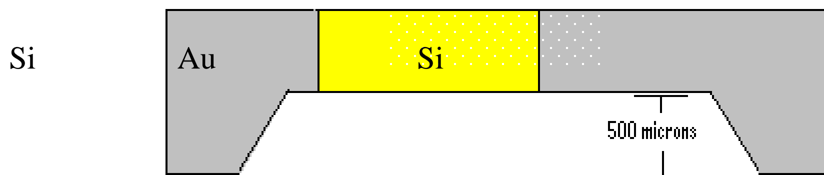

Figure 9: Schematic of backside wet etching with KOH.

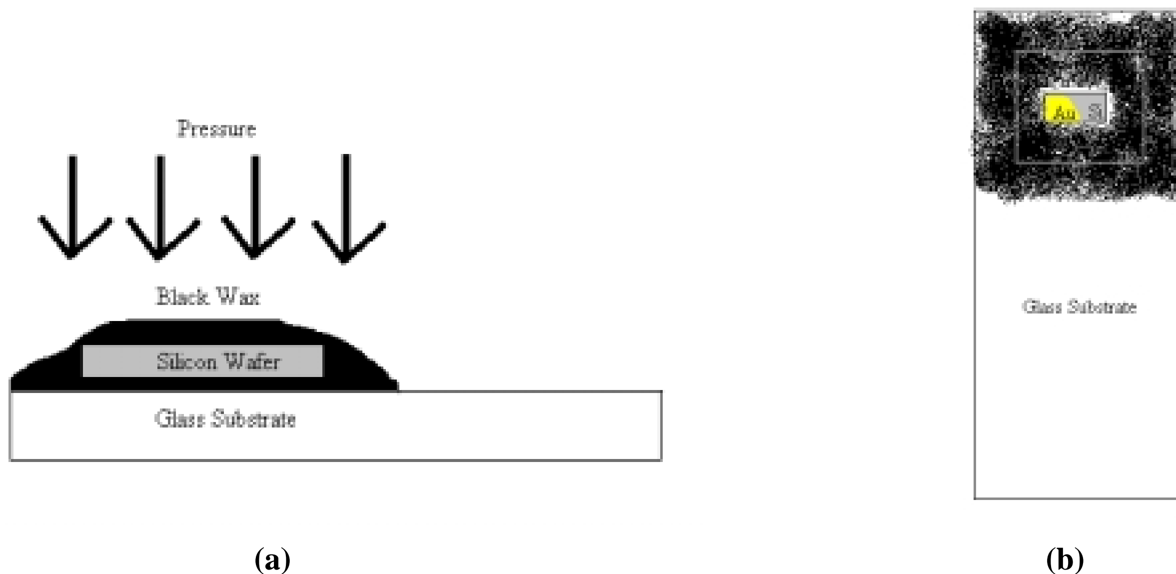

Figure 10: (a) Side view showing method for applying black wax; (b) front view showing window to be chemically etched.

3. EXPERIMENTAL RESULTS AND DISCUSSION

3.1 Morphology of Electrodeposits

One of the goals in the microfabrication process is to obtain high-resolution morphology - uniform grain size, constant film thickness, and smooth texture - from electroplating. Although literature on metal deposition is extensive, research on electroplating for semiconductor and MEMS micromachining processes is only in the developmental stage. In the fabrication of compliant mechanisms such as ETC microactuators, poor morphology can have a negative impact on performance. Finite element analysis of such devices has shown that the thermal (e.g., convection, radiation, and conduction) boundary conditions of compliant mechanisms are dependent on the surface conditions of the material [8]. In addition, poor morphology, notably non-uniform and large grain size of gold deposits, is believed to create thermal stress during expansion and contraction of the gold thin film [2]. Moreover, we have found that gold films with coarse grain size variations evidently have more porous deposits than ones with fine grain sizes.

Typically, compliant structures need to be built with materials whose stress-strain relations are predictable and can be modeled in at least one direction. This requirement demands uniform stress distribution in materials (e.g., silicon fulfills this requirement). Thus, non-uniform grain sizes can make the performance of compliant mechanisms incompatible with the predictions made from topology optimization. The reliability of a compliant mechanism is as important as improving the performance of compliant MEMS devices. Having proper structural and surface morphology is a major concern for designers and researchers.

In all the parameters tested, current density variations have the largest effect on deposition morphology and rate. Using a profilometer and a low-power microscope, we are able to tell that

lower-current-density applications reduce porous “spongy” deposits, improve surface topography, and create finer sizes of deposits than high-current-density ones. At high-current applications - i.e., 5 and 10 mA - the profile of the deposit contains more sharp and lofty peaks. The scanning electron microscope pictures in Figure 11 compare gold deposits at a high-current density to deposits at low-current density. We examine the profile of each deposit before the cavity is completely filled with gold. We find that surface roughness increases as deposition proceeds, meaning this morphological factor is time-dependent.

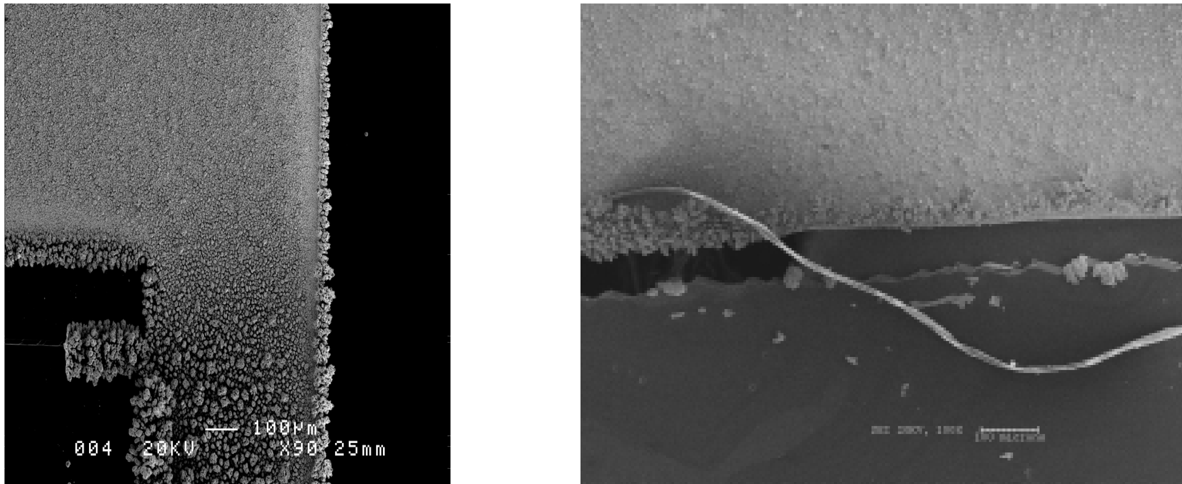

(a) (b)

Figure 11a and 11b: SEM photographs that show gold and silicon side-by-side. (a) Electroplating at high-current density (10 mA) – 90x magnification. (b) Electroplating at low-current density (2 mA) – 100x magnification.

The surface morphology of 5 and 10 mA specimens also displayed obvious characteristics of dendrites and porosity, but the 2 and 3.3 mA cases did not. Dendrites are preferential growths of deposits protruding in one area. In our research, the growth of dendrites seems to be more prolific with increasing current density. Porous deposits are another electrodeposit phase to be avoided in fabricating compliant micromechanisms. Popov and Krstajic have shown that spongy growth is dependent on the overpotential of the electroplating process [17]. Their research shows that increasing the voltage increases the total current but not the current used for electroplating. The excess current stimulates hydrogen evolution instead and creates the porous metal deposits.

3.2 Hydrogen Evolution

Hydrogen evolution during electroplating should be avoided. One reason is that hydrogen bubbles evolved can block the surface that is being electroplated, thus decreasing the electroplated area. Most significantly, hydrogen gas evolution decreases the current efficiency for the reason discussed earlier. The reason the wafer clamps need to be above the electrolyte is also to avoid hydrogen gas production. That is, there is an increase of hydrogen gas evolution when the clamps are down, thus directly electrolyzing the water in the gold solution, which can

significantly lower the current efficiency at the cathode. In the typical chemical reactions that occur in the solution, hydrogen can be released as a gas or discharged as H^+ ions. These additional ions can also change the pH of the solution. Hence, controlling hydrogen gas or ion creation can be complicated.

Using a microscope, we noticed small cracks on the surface of the gold surface. They can be explained by the following conjecture: When the bonds of hydrogen break in the discharge of H^+, some of the energy is released into the solution and some of it is absorbed by the 20-µm gold film and silicon substrate, since most of the hydrogen bubbles erupt from the edges and surface of the deposit [13]. Consequently, there is a buildup of fracture-induced thermal stress on the gold film surface. As examined, hydrogen evolution can have detrimental effects on the performance of electrodeposition.

One other major reason that lower-current density is preferred over high density is because experimental results show that hydrogen evolution is linked to higher-current densities. At current applications below 2mA, we did not see the hydrogen bubbles with the naked eye; however, above 3 mA, we easily saw the bubbles erupting from the surface of the gold film, especially near the edges of the cavity.

3.3 Electrodeposition Rate Dependence on Current Density

At 1 mA, plating did not occur. This could be because the current applied probably did not supply enough power to overcome the activation overpotential. In other words, 1 mA current applications may not have overcome the reaction's activation energy barrier: primarily, driving the gold ions across the Helmholtz double layer to form the deposit. However, at 1 mA with stirring and heating, there was slight gold deposition over the cavity. Stirring of the gold solution is also believed to increase the effect of convective diffusion [12]. This is probably a result of the forced convective transport effects in the solution through the increment of random molecular collisions from heating and stirring. Also, the presence of a temperature gradient in the bulk region of the electrolyte that can give rise to heat transfer may explain why heating provides the necessary energy for the gold ions to migrate to the cavity on the substrate at 1 mA.

At 1.5 mA with stirring and heating up to 60° C, plating occurred, but the seed layer that provided electrical contact to the deposited cavity was removed during the electroplating process. However, the seed layers used for creating the necessary electrical contact remained strongly attached to the cavity throughout the fabrication process at room temperature. One reason the seed layer may not have adhered properly to the silicon substrate is that the additional stirring and heating may have disrupted its bonding to the silicon.

Table 1 and Figure 12 compare the experimental and theoretical deposition rates. In general, the experimental deposition rate increases with increasing current density, as does the theoretical deposition rate. The theoretical rate is calculated using Faraday's Law from equation (2), where the atomic weight and density of gold at 20° C are 196.96 and 19.32 g/cm^3, respectively, and the number of electrons transferred for the chemical reaction is 1. Using this comparison, the current efficiency at the cathode is also found. The current efficiency calculations correspond to the observations made on the hydrogen gas evolution — i.e., as the current density applied rises,

there is an increase in evolution of hydrogen gas. Therefore, hydrogen gas evolution does cause the current efficiency at the cathode to fall.

At 2mA, hydrogen gas evolution is minimized while the electroplating rate is maximized. Therefore, the optimum current density used for electroplating in this research is 2mA. Also, the best-electrodeposited morphology was obtained with this current density.

Table 1: Comparison of theoretical and experimental deposition rates.

Current Applied (mA)	Current Density (mA/cm^2)	Surface Morphology	Temperature (°C)	Experimental Deposition Rate (µm/hr)	Theoretical Deposition Rate Using Faraday's Law (µm/hr)	Current Efficiency α
1	1.9	Incomplete (insufficient current)	60	0	-----------------	--------------
1.5	2.9	Incomplete (seed layer peeled off)	60	-----------------	-----------------	--------------
2	3.7	Mediocre	20	14	14	~100%
3.3	6.4	Mediocre	20	13	24.3	53%
5	9.6	Poor	20	15	36.5	41%
10	19.2	Poor	20	32	73	43%

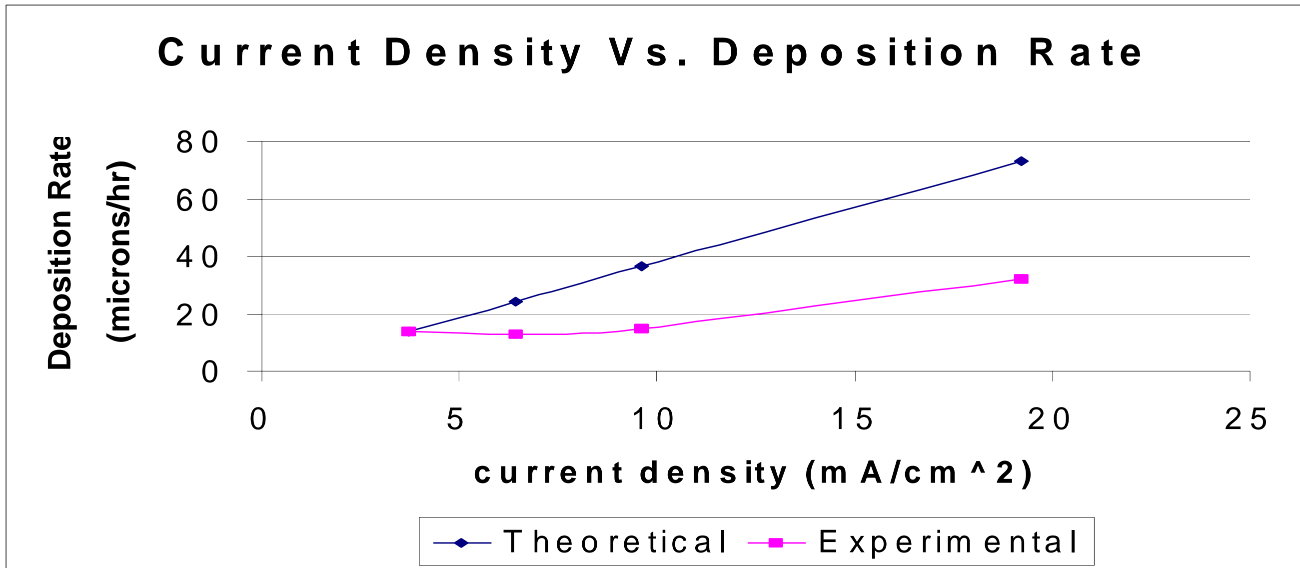

Figure 12: Graphical comparison of theoretical and experimental deposition rates.

3.4 KOH Etching

After the gold was deposited, the next step in the fabrication process was to etch the silicon wafer from the backside to release the structure. At ~30 % KOH by weight and about 65°C, we etched 500 μm of the silicon substrate at 0.56 μm/min. These are only approximate values given the limitations of the experimental procedure. We determined that etching the silicon substrate stopped at 500 μm because of the silicon dioxide layer (also known as the "oxide" layer) that is juxtaposed between two silicon layers. The oxide layer acts as the etch-stop layer; therefore, with this layer and the black wax protecting the back and front of the substrate, only the rectangle window exposed at the device layer surface will be anisotropically etched.

One disadvantage of using the anisotropic etchant KOH is that it etches the silicon dioxide layer at a high rate, depending on the etching conditions [12]. As a result, a thick silicon dioxide layer of 5 microns was chosen to be insulated between the SOI wafer in order to protect and mask the backside of the silicon substrate prior the 500-μm-deep etch with KOH.

Although we etched 500 microns of the silicon substrate, but releasing the structure to form a cantilever beam or compliant mechanism that can be actuated is yet complete. Due to the phenomena of stiction, where the glass substrate adheres naturally to the silicon surface, the partially released structure shown in Figure 9 collapsed. Stiction is a common problem found in MEMS fabrication processes, where surface tension created from the KOH solution, causes the silicon surface to stick on to the glass substrate [12]. When surface tension decreases from water rinsing procedures, and as the ~25 micron structure is about to detach from the glass substrate, cracking is believed to develop in the thin silicon film. The cracking of the film may also be linked to extrinsic film stresses such as thermal stresses, where external factors such as temperature gradients can cause inhomogeneous CTE subjected to temperature changes during the KOH etching process. Because failure of the mechanical structure can be a yield-limiting step in the fabrication process, more research needs to be done to improve the novel anisotropic wet etching procedures.

4. CONCLUSION

Although we never finished manufacturing a compliant device, the new fabrication process consisting of MEMS micromachining techniques followed by electroplating, appears promising. With electroplating, two materials can be easily placed side-by-side on the same plane. By adjusting the plating parameters, one can also optimize the morphology of the metal deposits with careful monitoring of plating conditions.

In summary, we found out that the magnitude of the overpotential, which depends strictly on the current density of a chemical reaction, can determine the electroplating rate and the morphology of the electrodeposit. Although minimizing the overpotential is goal of electroplating method, but lowering the current density below the limiting current density can be a problem. With too low of a current density, the electroplating will not operate. Therefore, maximizing the reaction kinetics by heating and stirring can drive the chemical reactions in an electrochemical cell when the current density is too low.

Even upon completion of a two-material compliant mechanism, electrothermally actuating it poses problems – i.e., at high temperatures, gold can diffuse into silicon and gold may not adhere properly to the silicon. Therefore, understanding the material response of the compliant mechanism during actuation is important. It can help improve the design of the mechanism as well as enable one to predict the capability of such a device.

5. RECOMMENDATIONS

Pulse plating of metals has long been known to avoid many of the morphology problems associated with potentiostatic and galvanostatic plating [13]. Numerous experiments on electrodeposition have shown that despite the few advantages in galvanostatic plating, pulse plating is a better technique for electroplating. Past research has shown that pulse plating does not require a continuous voltage or current application; thus, reducing surface roughness, porosity, and edge thickness buildup when compared to dc plating [18]. However, a recent paper on metal deposition contradicts the traditional standpoint that pulse plating is a better micromachining technique than dc plating [18]. That research actually found improved morphology with dc plating. Therefore, in future work, more research needs to be done in this area as well.

6. ACKNOWLEDGMENTS

I would first like to thank the National Science Foundation for their sponsorship of undergraduate research through the SUNFEST-REU program and to express my gratitude to Vladimir Dominko for his help and guidance. Finally, and most importantly, I would like to thank Dr. Ananthasuresh, Jun Li, and their group for giving me this wonderful opportunity as well as inspiring me throughout an exciting journey.

7. REFERENCES

[1] O. Sigmund, Systematic design and optimization of multi-material, multi-degree-of-freedom microactuators, *Proc. MSM 2000*, San Diego, CA, USA, March 27-29, 2000, pp. 36-49.

[2] W. Ruythooren, K. Attenborough, S. Beerten, P. Merken, J. Fransaer, E. Beyne, C. Van Hoof, J. De Boek, and J.P. Celis, Electrodeposition for the synthesis of microsystems, *J. Micromech. Microeng.,* 10 (2000), pp. 101 -107.

[3] T. Moulton and G. K. Ananthasuresh, Micromechanical devices with embedded electro-thermal-compliant actuation, *Sensors and Actuators - A*, 90 (2001), pp. 38-48.

[4] http://www.s3.kth.se/mst/research/dissertations/pdf/thorbjornelic.pdf (accessed 7/26/01)

[5] W. Riethmuller and W. Benecke, Thermally excited silicon microactuators, *IEEE Trans. Electron Devices*, 35 (1988), pp. 758 - 762.

[6] G. T. A. Kovacs, *Micromachined Transducers Sourcebook*, McGraw-Hill, New York, 1998, pp. 91, 105, 289, 292.

[7] T. Moulton, Analysis and design of electro-thermal-compliant microdevices, Center for Sensor Technologies at the University of Pennsylvania Technical Report # TR-CST31DEC97, 1997, pp. 13-26.

[8 N. D Mankame and G. K. Ananthasuresh, The effect of thermal boundary conditions and scale on the behavior of electro-thermal-compliant micromechanisms, *Proc. MSM 2000*, San Diego, CA, USA, March 27-29, 2000, pp. 257-260.
[9] J. Jonsmann, O. Sigmund, and S. Bouwstra, Compliant electro-thermal microactuators, *MEMS '99*, 1999, pp. 588-593.
[10] L. Yin and G. K. Ananthasuresh, A new material interpolation scheme for the topology optimization of thermally actuated compliant micromechanisms, (in press)
[11] L. Yin and G. K. Ananthasuresh, Topology of compliant mechanisms with multiple materials using a peak function material interpolation scheme, *Structural and Multidisciplinary Optimization* (in press).
[12] M. Madou, *Fundamentals of Microfabrication*, CRC Press, New York, 1997, pp. 97, 118-124.
[13] R.K. Pandey, S.N Sahu, and S. Chandra, *Handbook of Semiconductor Electrodeposition*, Marcel Dekker, Inc., New York, 1996, pp. 2-19, 29-36, 60, 82-85,115-119.
[14] http://www.ece.gatech.edu/research/labs/vc/packaging (accessed 7/18/01)
[15] D.P. Seraphim, R. Lasky, and C-Y Li., *Principles of Electronic Packaging*, McGraw-Hill, New York, 1989, pp. 470-518.
[16] http://www.chem.uiuc.edu/demos/elec.html (accessed 7/31/01)
[17] K. I. Popov and N. V. Krstajic, *J. Appl. Electrochemical,* 13 (1983) p.775.
[18] J-M Quemper, E. Dufour-Gergam, N. Frantz-Rodriquez, J-P Gilles, J-P Grandchamp and A. Bosseboeuf, Effects of direct and pulse current on copper electrodeposition through photoresists mold, *J. Micromech. Microeng.*, 10 (2000), pp. 116 -119.